Supplementary Information (SI) for CrystEngComm.

N-iodophtalimide as halogen bond donor, a comparison with N-iodosuccinimide and N-iodosaccharin

Ie-Rang Jeon, Olivier Jeannin, Frédéric Barrière, Antoine Robert and Marc Fourmigué*

UnivRennes, CNRS, ISCR (Institut des Sciences Chimiques de Rennes), Campus de Beaulieu, Rennes, 35000, France

SUPPLEMENTARY INFORMATION

1. Synthesis and crystal growth

Reagents were obtained from commercial suppliers and used without further purification. Solvents were dried using commercial solvent purification system from Inert Technology.

Synthesis.

N-iodophthalimide (NIPht).[1] Phthalimide (1 g, 6.8 mmol), $PhI(OAc)_2$ (1.05g, 3.26 mmol) and diiodine (0.9 g, 3.55 mmol) are dissolved in CH_3CN (30 mL). The reaction mixture is then stirred at RT overnight. The yellow solution is then concentrated under reduced pressure. The yellow oil is dispersed in CCl_4 (30 mL) and stirred at 0°C during 15 min. The precipitate is filtered and the white solid washed with cold CCl_4 and dried under vacuum (1.83 g, 6.72 mmol, 99% yield). ^1H NMR (300 MHz, CD_3CN) δ_H = 7.75 (m, 4H). Crystals were obtained from CH_2Cl_2/hexane.

Co-crystal preparations

(NIPht)•DMAP. NIPht (7.0 mg, 0.026 mmol) and 4-dimethylaminopyridine (DMAP, 6.5 mg, 0.053 mmol) were solubilized in DCM (10 mL). Diffusion of pentane vapor into the DCM solution at ambient temperature afforded colorless block-shaped crystals suitable for single-crystal X-ray diffraction after 2 weeks.

α-(NIPht)$_2$(*p*-bipy). NIPht (6.0 mg, 0.022 mmol) and 4,4'-bipyridine (2.0 mg, 0.0013 mmol) were solubilized in DCM (1 mL). Diffusion of pentane vapor into the DCM solution at ambient temperature afforded colorless prism-shaped crystals suitable for single-crystal X-ray diffraction after 3 weeks.

β-(NIPht)$_2$(*p*-bipy). NIPht (4.0 mg, 0.015 mmol) and 4,4'-bipyridine (50 mg, 0.013 mmol) were solubilized in DCM (10 mL). Layering of pentane (10 mL) over the DCM solution at 4°C afforded colorless prism-shaped crystals suitable for single-crystal X-ray diffraction after 2 weeks.

(NISacc)$_2$(*p*-bipy). NISacc (7.5 mg, 0.024 mmol) and 4,4'-bipyridine (16 mg, 0.010 mmol) were solubilized in DCM (1 mL). The resulting mixture was filtered through celite to remove insoluble residues. Layering of hexane (1 mL) over the filtrate at ambient temperature afforded colorless prism-shaped crystals suitable for single-crystal X-ray diffraction after 1 week.

(NIPht)$_2$(*o*-bipy). NIPht (6.8 mg, 0.025 mmol) and 2,2'-bipyridine (16 mg, 0.010 mmol) were solubilized in DCM (1.5 mL). The resulting mixture was filtered through celite to

remove insoluble residues. Layering of hexane (2 mL) over the filtrate at 4°C afforded colorless prism-shaped crystals. Despite several trials, the quality of the X-ray data collection was too poor to allow for a complete refinement. The compound crystallizes in the triclinic system, space group P1, with two crystallographically independent $(NIPht)_2$(*o*-bipy*)* adducts in the unit cell. They both exhibit structural characteristics closely related to those observed in the analogous *o*-Me_2bipy analog. Crystal data: $C_{26}H_{16}I_2N_4O_4$, M = 702.23 g mol^{-1}, triclinic, space group P1, a = 4.105(2), b = 14.432(6), c = 21.013(9) Å, α = 89.234(12), β = 84.512(15), γ = 81.820(14)°, *V* =1226.6(9) $Å^3$, Z = 2, T = 296(2) K.

$(NIPht)_2$(*o*-Me_2bipy). NIPht (6.0 mg, 0.022 mmol) and 5,5'-dimethyl-2,2'-bipyridine (2 mg, 0.011 mmol) were solubilized in DCM (6 mL). Diffusion of pentane vapor into the DCM solution at ambient temperature afforded colorless prism-shaped crystals suitable for single-crystal X-ray diffraction after 10 days.

$(NISucc)_2$(*o*-bipy). NISucc (11.3 mg, 0.050 mmol) and 2,2'-bipyridine (4.0 mg, 0.026 mmol) were solubilized in DCM (5 mL). Diffusion of pentane vapor into the DCM solution at ambient temperature afforded colorless needle-shaped crystals suitable for single-crystal X-ray diffraction after 2 weeks.

$(NISucc)_2$(*o*-Me_2bipy). NISucc (13.5 mg, 0.060 mmol) and 5,5'-dimethyl-2,2'-bipyridine (5.7 mg, 0.031 mmol) were solubilized in DCM (6 mL). Layering of pentane over the DCM solution at 4°C afforded colorless needle-shaped crystals suitable for single-crystal X-ray diffraction after 2 weeks.

$(NISacc)_2$(*o*-bipy). NISacc (3.0 mg, 0.010 mmol) and 2,2'-bipyridine (1 mg, 0.006 mmol) were solubilized in DCM (6 mL). Layering of pentane (6 mL) over the DCM solution at 4°C afforded colorless prism-shaped crystals suitable for single-crystal X-ray diffraction after 1 month.

[K(18-crown-6)](phthalimide)•*N*-iodophthalimide. NIPht (30 mg, 0.110 mmol), potassium phthalimide (30 mg, 0.162 mmol) and 18-crown-6 (42 mg, 0.159 mmol) were solubilized in DCM (1 mL). The resulting mixture was filtered through Celite to remove insoluble residues. Layering of hexane (2 mL) over the filtrate at 4°C afforded colorless prism-shaped crystals suitable for single-crystal X-ray diffraction after 1 week.

2. Crystallographic studies

Table S1. Crystallographic data[a,b]

	NIPht	**(NIPht)•DMAP**	**α-(NIPht)$_2$(*p*-bipy)**
CCDC	2366101	2366102	2366103
Formulae	$C_8H_4INO_2$	$C_{15}H_{14}IN_3O_2$	$C_{26}H_{16}I_2N_4O_4$
FW (g.mol^{-1})	273.02	395.19	702.23
System	orthorhombic	monoclinic	monoclinic
Space group	$P2_12_12_1$	$P2_1/n$	$P2_1/n$
a (Å)	4.9049(2)	9.2802(9)	4.8622(3)
b (Å)	7.0364(2)	11.8980(11)	33.380(3)
c (Å)	24.1144(8)	13.5467(11)	8.0329(5)
α (deg)	90.00	90.00	90.00
β (deg)	90.00	100.135(3)	104.989(3)
γ (deg)	90.00	90.00	90.00
V (Å^3)	832.26(5)	1472.4(2)	1259.38(16)
T (K)	296(2)	150(2)	296(2)
Z	4	4	2
Cryst. dim. (mm)	0.14×0.06×0.04	0.14×0.08×0.04	0.24×0.08×0.01
D_{calc} (g.cm^{-3})	2.179	1.783	1.852
μ (mm^{-1})	3.801	2.183	2.537
Absorption corr.	multi-scan	multi-scan	multi-scan
T_{min}, T_{max}	0.761, 0.859	0.811, 0.916	0.784, 0.975
Total refls	5953	20445	6306
Uniq refls (R_{int})	1914 (0.027)	3308 (0.0249)	2870 (0.0345)
Uniq refls (I > 2σ(I))	1807	3086	2178
R_1, wR_2	0.0271, 0.0559	0.016, 0.0381	0.0447, 0.0777
R_1, wR_2 (all data)	0.0297, 0.0572	0.0182, 0.0399	0.0669, 0.0838
GOF	1.069	1.115	1.043

[a] $R_1 = ||F_o| - |F_c||/|F_o|$. [b] $wR_2 = [w(F_o^2 - F_c^2)^2]/[w(F_{o2})^2]^{1/2}$.

Table S1 (continued). Crystallographic data[a,b]

	β-(NIPht)$_2$(*p*-bipy)	**(NIPht)$_2$(*o*-Me$_2$bipy), CH$_2$Cl$_2$**	**(NISacc)$_2$(*p*-bipy)**
CCDC	2366104	2366105	2366106
Formulae	$C_{26}H_{16}I_2N_4O_4$	$C_{29}H_{22}Cl_2I_2N_4O_4$	$C_{24}H_{16}I_2N_4O_6S_2$
FW (g.mol^{-1})	702.23	815.21	774.33
System	monoclinic	orthorhombic	monoclinic
Space group	*P*2$_1$/c	*P*ba2	*P*2$_1$/c
a (Å)	7.5392(8)	25.6531(16)	8.6873(9)
b (Å)	9.4310(10)	14.2270(8)	9.2187(10)
c (Å)	17.2253(18)	4.1646(3)	16.9914(16)
α (deg)	90.00	90.00	90.00
β (deg)	97.896(3)	90.00	105.954(3)
γ (deg)	90.00	90.00	90.00
V (Å^3)	1213.1(2)	1519.94(17)	1308.4(2)
T (K)	296(2)	296(2)	296(2)
Z	2	2	2
Cryst. dim. (mm)	0.10×0.09×0.03	0.23×0.08×0.04	0.23×0.18×0.12
D_{calc} (g.cm^{-3})	1.922	1.781	1.966
μ (mm^{-1})	2.634	2.286	2.611
Absorption corr.	multi-scan	multi-scan	multi-scan
T_{min}, T_{max}	0.768, 0.924	0.817, 0.919	0.575, 0.731
Total refls	2727	13219	28084
Uniq refls (R_{int})	2727 (0.048)	3449 (0.0542)	28084 (0.0553)
Uniq refls (I > 2σ(I))	2216	2655	22562
R_1, wR_2	0.0374, 0.0726	0.040, 0.0759	0.0324, 0.0732
R_1, wR_2 (all data)	0.0563, 0.0788	0.0618, 0.0818	0.0474, 0.0828
GOF	1.188	1.061	0.907

[a] $R_1 = ||F_o| - |F_c||/|F_o|$. [b] $wR_2 = [w(F_o^2 - F_c^2)^2]/[w(F_{o2})^2]^{1/2}$.

Table S1 (continued). Crystallographic data[a,b]

	(NISucc)$_2$(*o*-bipy)	**(NISucc)$_2$(*o*-Me$_2$bipy)**	**(NISacc)$_2$(*o*-bipy)**
CCDC	2366107	2366108	2366109
Formulae	$C_{18}H_{16}I_2N_4O_4$	$C_{20}H_{20}I_2N_4O_4$	$C_{24}H_{16}I_2N_4O_6S_2$
FW (g.mol^{-1})	606.15	634.2	774.33
System	monoclinic	monoclinic	triclinic
Space group	$P2_1/c$	$P2_1/c$	$P\bar{1}$
a (Å)	21.488(2)	8.4092(8)	8.0405(6)
b (Å)	10.0888(8)	16.8459(18)	12.0158(8)
c (Å)	9.4428(9)	15.5232(16)	17.3956(12)
α (deg)	90.00	90.00	94.170(2)
β (deg)	90.324(3)	94.164(4)	102.710(2)
γ (deg)	90.00	90.00	105.874(2)
V (Å^3)	2047.1(3)	2193.2(4)	1561.04(19)
T (K)	150(2)	150(2)	296(2)
Z	4	4	2
Cryst. dim. (mm)	0.11×0.08×0.04	0.19×0.08×0.02	0.25×0.08×0.02
D_{calc} (g.cm^{-3})	1.967	1.921	1.647
μ (mm^{-1})	3.104	2.902	2.189
Absorption corr.	multi-scan	multi-scan	multi-scan
T_{min}, T_{max}	0.742, 0.883	0.757, 0.944	0.810, 0.957
Total refls	26687	37649	19283
Uniq refls (R_{int})	4638 (0.0247)	5000 (0.0367)	7101 (0.0444)
Uniq refls (I > 2σ(I))	4525	4791	4889
R_1, wR_2	0.0206, 0.0444	0.0173, 0.0428	0.0423, 0.0946
R_1, wR_2 (all data)	0.0213, 0.0447	0.0183, 0.0439	0.0725, 0.1054
GOF	1.197	0.720	1.021

[a] $R_1 = ||F_o| - |F_c||/|F_o|$. [b] $wR_2 = [w(F_o^2 - F_c^2)^2]/[w(F_{o2})^2]^{1/2}$.

Table S1 (continued). Crystallographic data[a,b]

	[K(18-c-6)][NPht–I–NPht]
CCDC	2366110
Formulae	C28 H32 I K N2 O10
FW (g.mol^{-1})	722.55
System	triclinic
Space group	$P\bar{1}$
a (Å)	9.9210(19)
b (Å)	11.407(3)
c (Å)	16.152(3)
α (deg)	102.724(8)
β (deg)	99.561(7)
γ (deg)	114.396(7)
V (Å^3)	1554.3(6)
T (K)	296(2)
Z	2
Cryst. dim. (mm)	0.34×0.10×0.08
D_{calc} (g.cm^{-3})	1.544
μ (mm^{-1})	1.221
Absorption corr.	multi-scan
T_{min}, T_{max}	0.864, 0.907
Total refls	10644
Uniq refls (R_{int})	6707 (0.022)
Uniq refls (I > 2σ(I))	5270
R_1, wR_2	0.0389, 0.0855
R_1, wR_2 (all data)	0.0566, 0.0954
GOF	1.042

[a] $R_1 = ||F_o| - |F_c||/|F_o|$. [b] $wR_2 = [w(F_o^2 - F_c^2)^2]/[w(F_{o2})^2]^{1/2}$.

3. Theoretical calculations

DFT geometry optimizations of molecules or adducts were carried out as reported by Taylor *et al.*[2] using Gaussian 16 Revision A.03.[3] Namely, the B3LYP functional and the 6-31+G** basis set for all atoms and the LANLdp basis set for iodine were used together with the default convergence criteria implemented in the program. GaussView 6.0.16 was used to generate figures.

(a)

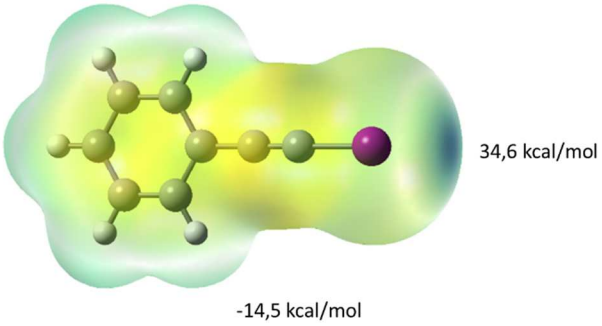

(b)

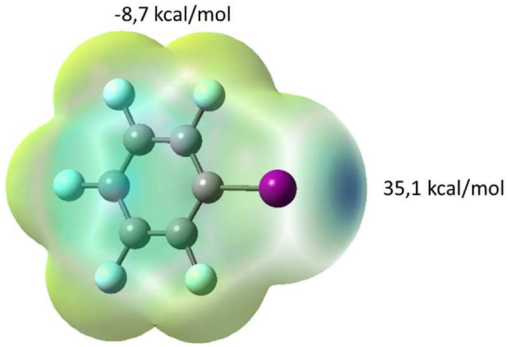

Fig. S1 Molecular electrostatic potential surface at an isovalue of 0.001 of (a) Ph–C≡C–I and (b) C_6F_5–I (B3LYP/6-31G**-LANLdp, Gaussian16) with extrema values indicated. Red indicates negative charge density and blue positive charge density. The full-scale range similar to the one used in Fig. 3, i.e. –0.0522/+0.0725 au (Hartrees), i.e. –32.8/+45.5 kcal/mol.

4. Complementary structural data

(a)

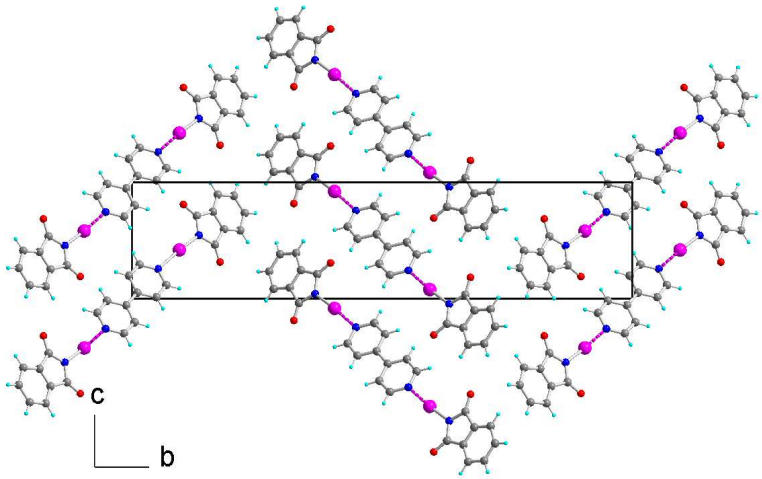

(b)

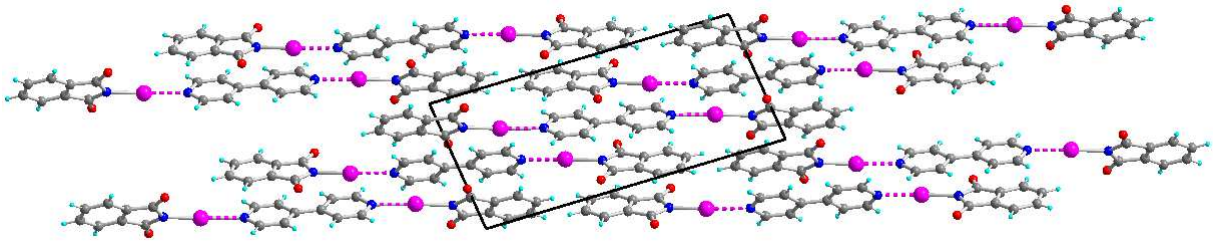

Fig. S2 Solid state organization of (a) α-(NIPht)$_2$(*p*-bipy) adduct, and (b) β-(NIPht)$_2$(*p*-bipy)

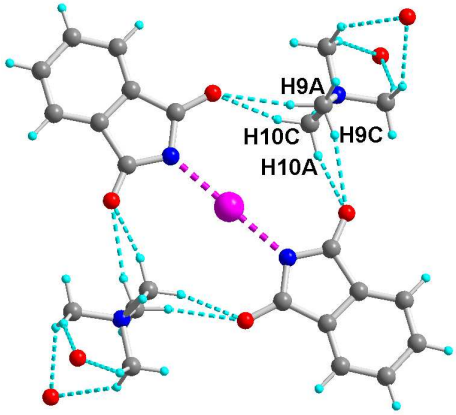

Fig. S3 Detail of the C–H•••O HB interactions (cyan dotted lines) in [Me$_4$N][NPht–I–NPht].

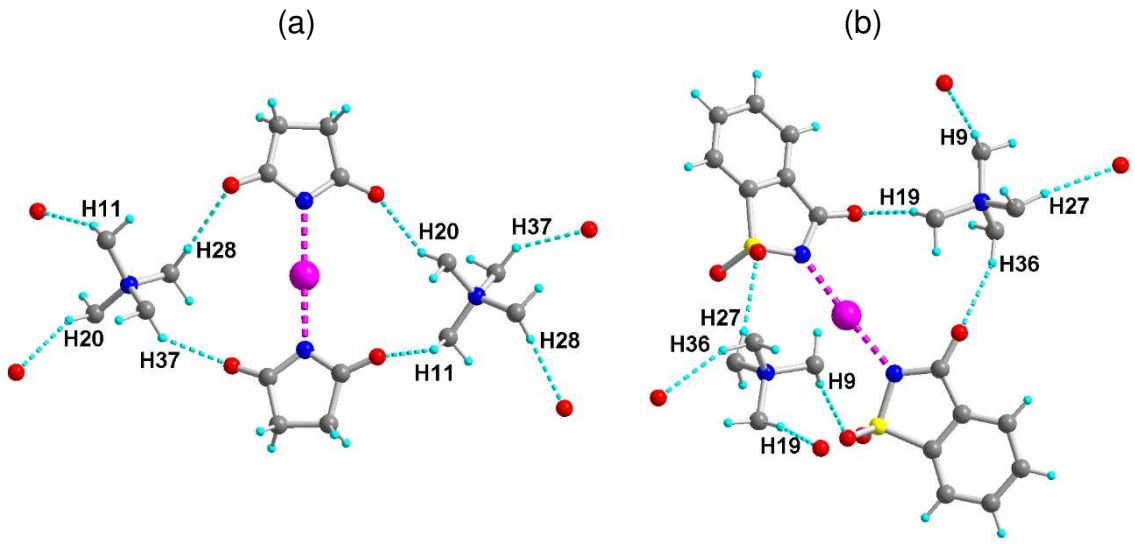

Fig. S4 Details of the C–H•••O HB interactions (cyan dotted lines) in (a) [Bu_4N][NSucc–I–NSucc] and (b) [Bu_4N][NSacc–I–NSacc]. Only the α-methylene groups of the Bu_4N^+ cations are shown for clarity.

Table S2 Structural characteristics of the C–H•••O hydrogen bond interactions in [Me_4N][NPht–I–NPht], [Bu_4N][NSucc–I–NSucc] and [Bu_4N][NSacc–I–NSacc]. See Figs. S3 and S4 for hydrogen atom numbering.

	H•••O dist. (Å)	C–H•••O ang. (°)	Ref.
[Me_4N][NPht–I–NPht]			4
C9–H9A•••O2	2.481(10)	153.96(74)	
C9–H9C•••O1	2.447(16)	144.87(87)	
C10–H10A•••O1	2.522(11)	144.83(73)	
C10–H10C•••O2	2.413(14)	156.40(81)	
[Bu_4N][NSucc–I–NSucc]			5
C9–H11•••O2	2.322(2)	155.19(11)	
C13–H20•••O3	2.376(2)	150.0(1)	
C17–H28•••O4	2.382(1)	170.76(11)	
C21–H37•••O1	2.367(1)	144.62(10)	
[Bu_4N][NSacc–I–NSacc]			6
C15–H9•••O2	2.538(8)	167.88(22)	
C19–H19•••O4	2.538(4)	166.96(20)	
C23–H27•••O5	2.514(3)	174.39(21)	
C27–H36•••O1	2.468(3)	158.98(21)	

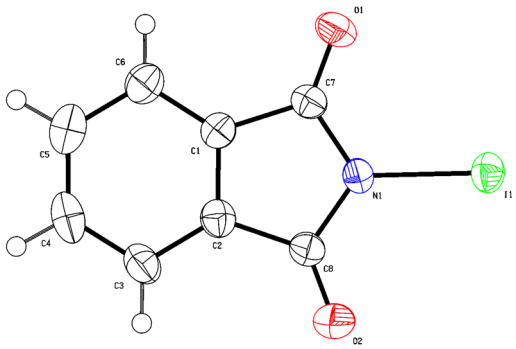

Fig. S5 ORTEP drawing for NIPht

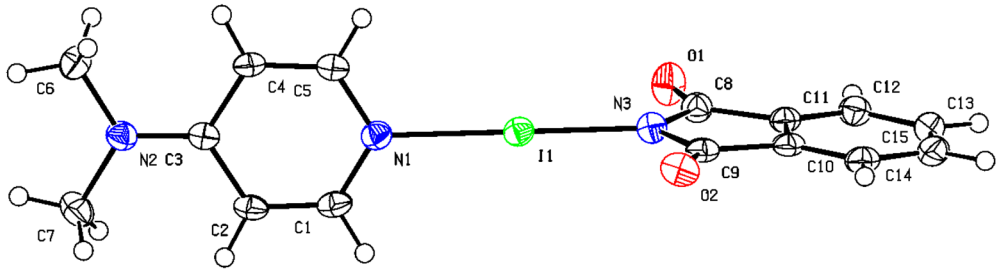

Fig. S6 ORTEP drawing for (NIPht)•DMAP

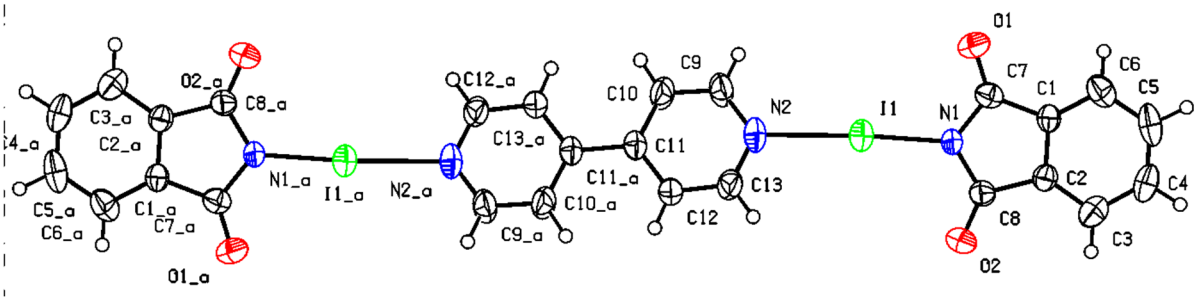

Fig. S7 ORTEP drawing for α-(NIPht)$_2$(*p*-bipy)

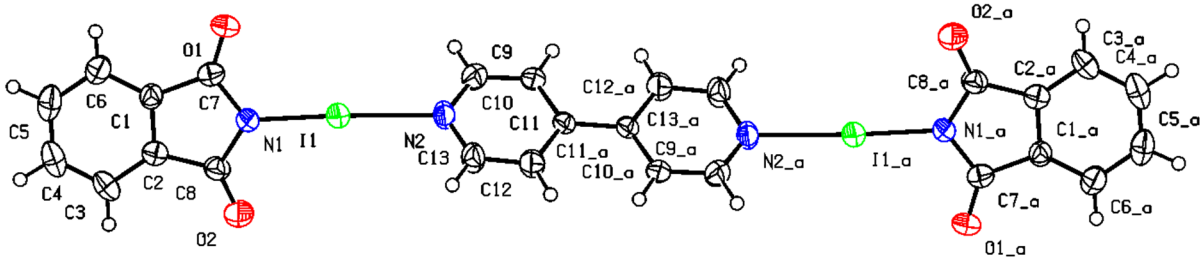

Fig. S8 ORTEP drawing for β-(NIPht)$_2$(*p*-bipy)

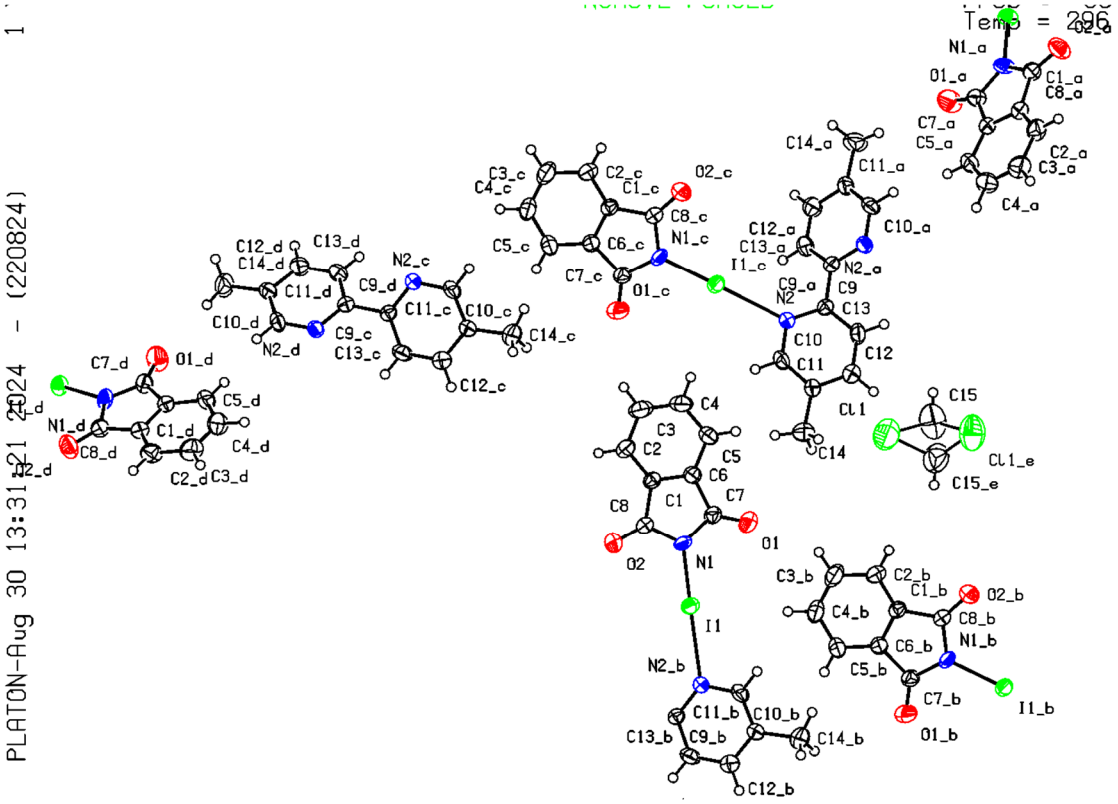

Fig. S9 ORTEP drawing for (NIPht)$_2$(*o*-Me$_2$bipy),CH_2Cl_2

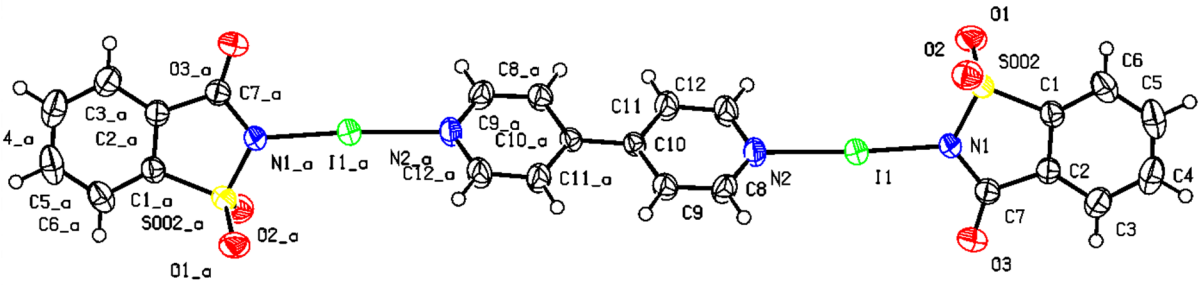

Fig. S10 ORTEP drawing for (NISacc)$_2$(*p*-bipy)

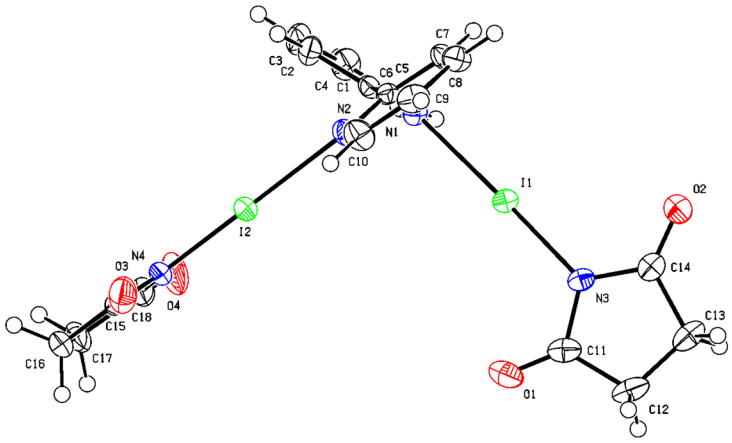

Fig. S11 ORTEP drawing for (NISucc)$_2$(*o*-bipy)

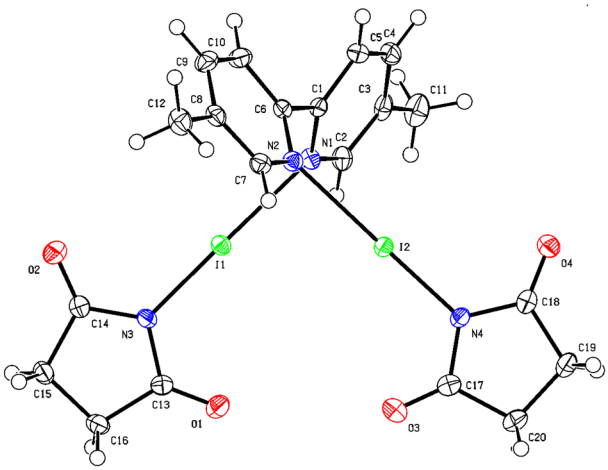

Fig. S12 ORTEP drawing for (NISucc)$_2$(*o*-Me$_2$bipy)

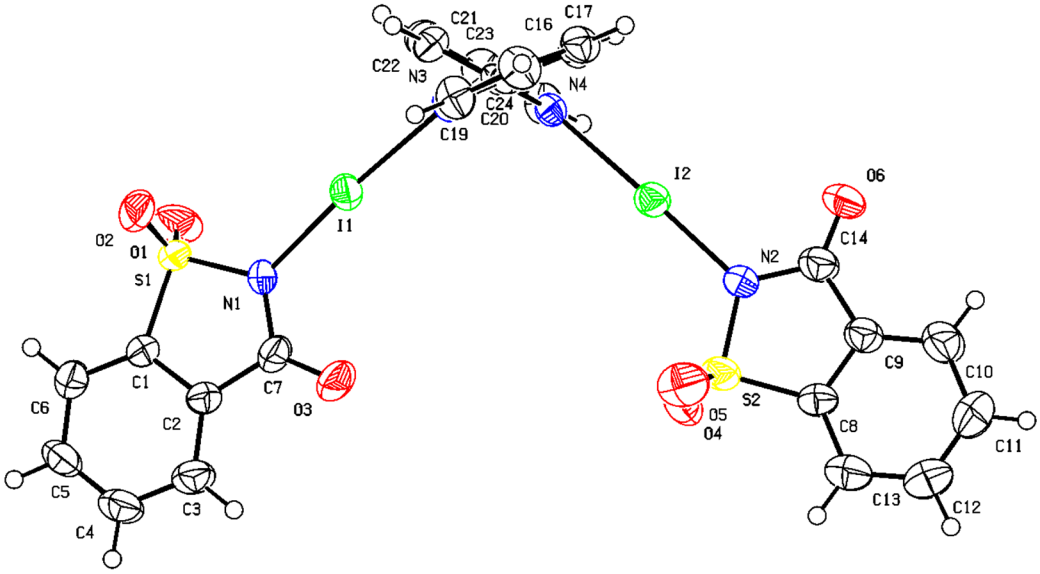

Fig. S13 ORTEP drawing for (NISacc)$_2$(*o*-bipy)

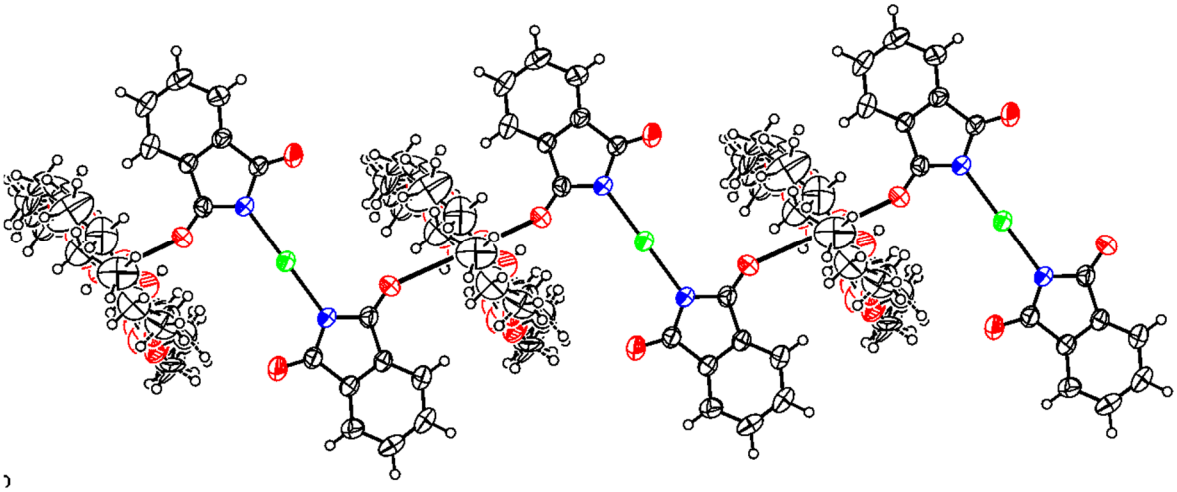

Fig. S14 ORTEP drawing for [K(18-c-6)][NPht–I–NPht]

References

[1] A. Artaryan, A. Mardyukov, K. Kulbitski, I. Avigdori, G. A. Nisnevich, P. R. Schreiner and M. Gandelman, *J. Org. Chem*., 2017, **82**, 7093–7100

[2] Sarwar, M. G.; Dragisic, B.; Salsberg, L. J.; Gouliaras, C.; Taylor, M. S. *J. Am. Chem. Soc*. **2010**, *132*, 1646–1653.

[3] Frisch, M. J.; Trucks, G. W.; Schlegel, H. B.; Scuseria, G. E.; Robb, M. A.; Cheeseman, J. R.; Scalmani, G.; Barone, V.; Petersson, G. A.; Nakatsuji, H.; Li, X.; Caricato, M.; Marenich, A. V.; Bloino, J.; Janesko, B. G.; Gomperts, R.; Mennucci, B.; Hratchian, H. P.; Ortiz, J. V.; Izmaylov, A. F.; Sonnenberg, J. L.; Williams-Young, D.; Ding, F.; Lipparini, F.; Egidi, F.; Goings, J.; Peng, B.; Petrone, A.; Henderson, T.; Ranasinghe, D.; Zakrzewski, V. G.; Gao, J.; Rega, N.; Zheng, G.; Liang, W.; Hada, M.; Ehara, M.; Toyota, K.; Fukuda, R.; Hasegawa, J.; Ishida, M.; Nakajima, T.; Honda, Y.; Kitao, O.; Nakai, H.; Vreven, T.; Throssell, K.; Montgomery, J. A., Jr.; Peralta, J. E.; Ogliaro, F.; Bearpark, M. J.; Heyd, J. J.; Brothers, E. N.; Kudin, K. N.; Staroverov, V. N.; Keith, T. A.; Kobayashi, R.; Normand, J.; Raghavachari, K.; Rendell, A. P.; Burant, J. C.; Iyengar, S. S.; Tomasi, J.; Cossi, M.; Millam, J. M.; Klene, M.; Adamo, C.; Cammi, R.; Ochterski, J. W.; Martin, R. L.; Morokuma, K.; Farkas, O.; Foresman, J. B.; Fox, D. J. Gaussian 16, Revision A03, Gaussian, Inc., Wallingford CT, 2016.

[4] S. Yu, K. N. Truong, M. Siepman, A. Siiri, C. Schumacher, J. S. Ward and K. Rissanen, *Cryst. Growth Des*., 2023, **23**, 662−669

[5] A. J. Guzmán Santiago, C. A. Brown, R. D. Sommer and E. A. Ison, *Dalton Trans*., 2020, **49**, 16166−16174

[6] N. Lucchetti, A. Tkacheva, S. Fantasia and K. Muñiz, *Adv. Synth. Catal*., 2018, **360**, 3889−3893